Dentomaxillofacial Radiology (2021) 50, 20210005

birpublications.org/dmfr

RESEARCH ARTICLE

Near-infrared reflection at 780 nm for detection of early proximal caries in posterior permanent teeth in vitro

Katrin Heck, Friederike Litzenburger, Thomas Geitl and Karl-Heinz Kunzelmann

Department of Conservative Dentistry and Periodontology, University Hospital, Ludwig-Maximilians-University Munich, Munich, Germany

Objectives: The aim of this *in vitro* study was to evaluate the diagnostic potential of near-infrared reflection at 780 nm ($NIRR_{780nm}$) for early proximal caries detection on the occlusal, buccal and oral surfaces of molars and premolars under simulated, clinically relevant conditions. The findings were validated by micro-computed tomography (μCT).
Methods: Bitewing radiography (BWR) was used as a comparative diagnostic method. 250 sound or decayed permanent teeth were examined using $NIRR_{780nm}$ and BWR. The $NIRR_{780nm}$ findings were evaluated using yes/no decisions depending on the presence of caries lesions, as the enamel-dentin junction was not detectable in the majority of samples. All $NIRR_{780nm}$, BWR and μCT findings were obtained twice by two trained examiners. $NIRR_{780nm}$ images were evaluated both occlusally alone and combined occlusally, lingually and buccally. All findings were presented in a cross-table. Sensitivity, specificity and area under the curve (AUC) values were calculated. Reliability assessment was performed using κ statistics.
Results: Underestimation of caries was observed for $NIRR_{780nm}$ in 26.0% of all surfaces and for BWR in 32.8% of all surfaces. Overestimation was 10.0% for $NIRR_{780nm}$ and 0.4% for BWR. Trilateral $NIRR_{780nm}$ assessment exhibited an overall accuracy of 67.2 %, an underestimation of 13.6% and an overestimation of 19.2%. Trilateral $NIRR_{780nm}$ exhibited 63.0% sensitivity and 69.6% specificity, while BWR exhibited 26.7% sensitivity but 100% specificity for proximal caries detection.
Conclusion: $NIRR_{780nm}$ is not suitable for reliable detection of early proximal caries, even with the application of an ideal setup and optimized *in vitro* conditions.
Dentomaxillofacial Radiology (2021) **50**, 20210005. doi: 10.1259/dmfr.20210005

Cite this article as: Heck K, Litzenburger F, Geitl T, Kunzelmann K-H. Near-infrared reflection at 780 nm for detection of early proximal caries in posterior permanent teeth in vitro. *Dentomaxillofac Radiol* 2021; **50**: 20210005.

Keywords: Dental caries; Diagnostic Imaging; Near-infrared light; X-ray microtomography; Sensitivity and specificity

Introduction

The treatment of proximal caries lesions is currently oriented towards prevention or minimally invasive treatment. Whereas only a few decades ago, caries therapy was mostly based on yes/no decisions regarding whether to drill and fill or to wait without treatment, today dentists have a wide range of therapies at their disposal. The process of finding a suitable therapy is multifactorial and is based on both patient- and tooth-related factors.[1,2] The established diagnostic method, visual examination combined with digital bitewing radiography (BWR), shows imperfect diagnostic accuracy for the early detection of proximal caries.[3–7] This is especially true for enamel lesions since these lesions are more difficult to detect in bitewing radiographs (BWRs) than dentin lesions due to their smaller size and lower loss of minerals.[8] Superimposition artefacts, as well as artefacts due to the anatomical shape of the teeth (*e.g.,* mesial indentation), result in weaker performance

Correspondence to: Dr Katrin Heck, E-mail: kheck@dent.med.uni-muenchen.de

Received 04 January 2021; revised 09 February 2021; accepted 10 February 2021

in the detection of enamel lesions in BWRs.[3] In addition, conventional X-rays expose the patient to ionizing radiation, which can have potentially harmful effects.[9] New optical diagnostic methods have the potential to significantly improve the diagnostic accuracy of caries detection, and new diagnostic devices can use near-infrared (NIR) light to reliably detect non-cavitated proximal caries without the disadvantages of ionizing radiation.[10–15] The NIR-based devices that are currently available typically use light in the 780–850 nm range, although *in vitro* studies using tooth sections have shown that using light at longer wavelengths (1050–1600 nm) provides better results.[16–18] The development of diagnostic devices with longer wavelength NIR light is hampered by cost, as diagnostic devices operating at 1050–1600 nm require special cameras with sensors made of indium-gallium-arsenide, and this considerably increases their cost.

It, therefore, makes sense to concentrate on lower wavelengths if less expensive cameras with silicon sensors are to be used. Although silicon sensor camera technology can theoretically process wavelengths up to 1000 nm, its quantum efficiency at 800 nm is only 50%, resulting in poorer image quality, especially at wavelengths exceeding 800 nm. For this reason, illumination with light of wavelength in the range of 800 nm appears to be a reasonable alternative for the development of diagnostic devices based on silicon sensors, although the results obtained using a commercial diagnostic camera based on near-infrared reflection (NIRR) at 850 nm did not yield satisfactory results in the detection of proximal caries.[15] Commercial devices, however, are not suitable for providing assistance in evaluating the physical principles on which they are based, since much of the essential information required is considered a trade secret. For example, there is no information about the lens system used or the image processing routines that are used to optimize the image quality.

Given this finding, the question arises as to the potential of NIRR (<800 nm) when used under optimized technical conditions, such as the use of an NIR camera with high-resolution, high-quality optical components and the observation of test samples from different angles. For this purpose, we developed an *in vitro* model that simulates realistic proximal contacts. To date, single teeth have usually been used to assess the diagnostic potential of optical diagnostic procedures.[10,11,15,19–22] However, single teeth are not a realistic option in regard to diagnosing proximal lesions under clinically relevant conditions.

Our study aimed to investigate the potential of NIRR for detecting early proximal caries and to determine whether the diagnostic results obtained using NIRR differ from those obtained using traditional digital X-ray bitewing imaging. Previous studies have indicated that the specificity of BWR ranging from 70 to 97% with a sensitivity between 24 and 42%. As BWR is the most commonly used diagnostic aid for caries detection in addition to visual examination, this method appeared to be a suitable standard for comparison with NIRR.[23] Therefore, the following two working hypotheses (H1) were formulated: first, shortwave NIRR (<800 nm) has the potential to detect early proximal caries lesions with high sensitivity and specificity (>70 %), and second, the diagnostic results obtained using NIRR (<800 nm) are comparable to the diagnostic results obtained using BWRs (sensitivity 24 to 42%, specificity 70 to 97%). Accordingly, the associated null hypotheses (H0) were as follows: shortwave NIRR (<800 nm) cannot detect early proximal caries lesions with high sensitivity and specificity above 70%, and NIRR (<800 nm) does not yield diagnostic results comparable to those achieved using BWR.

Methods and materials

Sample size

The sensitivity for the detection of enamel caries by NIRR is assumed to be 15%. Our goal was to increase this to 30%, with a power of greater than 90%, an α of less than 0.05 and an assumed caries prevalence of 50%.[15,23] Calculation of the sample size based on these parameters indicated that 250 samples were required.

Tooth selection and sample preparation

The protocol used in this *in vitro* study of anonymized dental specimens was accepted by the Ethics Committee of the Medical Faculty of the Ludwig-Maximilians-University of Munich (488-15 UE). 250 extracted permanent human molars and premolars were selected from a pool of teeth extracted from anonymous patients in the Munich area; the sampled teeth were not affected by any form of restoration, had no structural changes or damage other than caries lesions and visually showed fully matured roots. For preselection prior to micro-computed tomography (μCT) assessment, the mesial and distal surfaces of each specimen were observed in direct view and evaluated according to the International Caries Detection and Assessment System II (ICDAS II).[24] One proximal surface per sample tooth was integrated into the final sample to create a balanced distribution according to the sample size calculation of healthy and carious surfaces. A total of 131 healthy (ICDAS = 0) and 119 carious (ICDAS = 1–5) surfaces were included; of the carious teeth, 112 were enamel caries (1–3) and seven were dentin caries (4–5).

All samples were manually cleaned with scalers and supplied with an identification number (ID). The teeth were randomly combined into pairs using the "Random Numbers" function of MS Excel (Microsoft Excel 2016, Redmond, WA, USA), with each pair consisting of one tooth with an even numbered ID and one tooth with an odd numbered ID. The teeth were then fixed with composite (Luxatemp Star, DMG, Hamburg, Germany), with the lower half of the root in a 3D-printed specimen

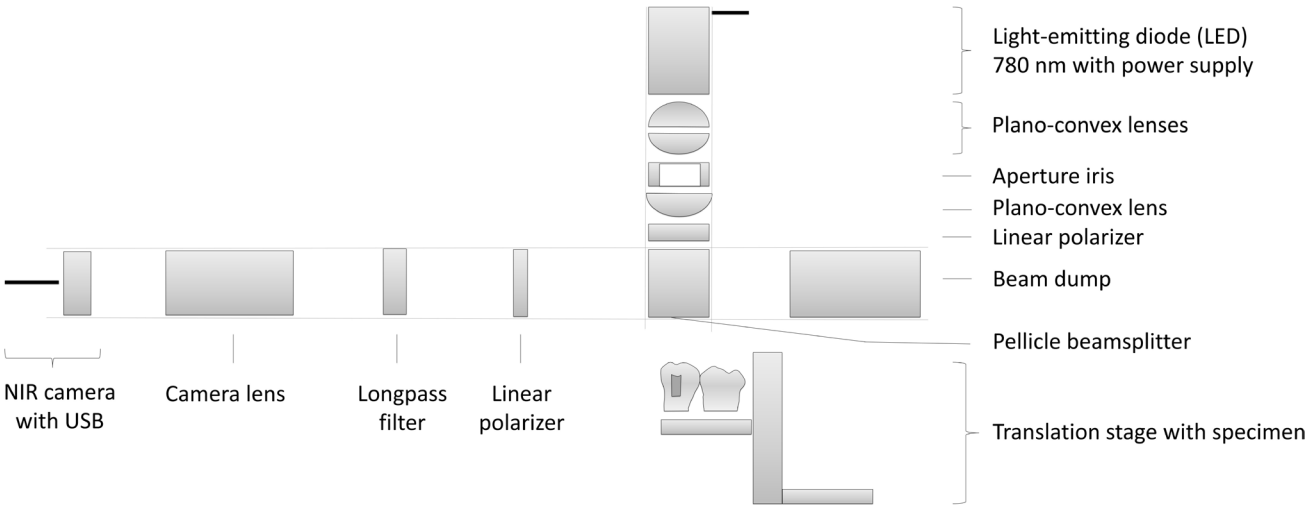

Figure 1 Schematic illustration of the NIRR in the *in vitro* model.

holder that was small enough to fit into the tomograph. Each holder was equipped with a male/female lock-and-key system and a magnet that was polymerized in the lower part of the container. The lock-and-key system made it possible to position the teeth in the same position relative to each other, and the magnets held the tooth samples securely together, ensuring reproducible proximal contact during the entire examination.[3] All teeth were stored in Ringer's solution containing 2% sodium azide at 4°C immediately after extraction and were removed from the storage boxes for approximately only five minutes to allow measurements to be made.

Near-infrared reflection images

A laboratory setup for NIRR measurements was developed on an optical breadboard (Figure 1). A light-emitting diode (LED) at 780 nm (M780L2-IR, Thorlabs, Newton, NJ, USA) was used as a light source. The LED was operated by a high-power LED driver (DC2100, Thorlabs) in continuous wave mode. The emitted light was focused by two plano-convex lenses that are anti-reflective (AR) over the range 650–1050 nm (LA1131-B, N-BK7 plano-convex lens, AR coating 650–1050 nm, diameter 1", focal length 50 mm, Thorlabs). An iris diaphragm was used to regulate the amount of emitted light entering the sample (SM1D12SZ, Thorlabs), followed by another plano-convex lens (LA1131-B, Thorlabs) to focus the light and a linear polarizer (LPNIRE100-B, linear polarizer with N-BK7, 600–1100 nm, Thorlabs) to reduce light reflections. The NIR light was then separated in a pellicle beam splitter (CM1-BP145B2, 700–900 nm, Thorlabs) at a ratio of 45 to 55; the larger portion of the light was diverted into a beam trap (BTC30, Thorlabs), and the smaller second beam was directed onto the specimen, which was attached to a translation stage (AP90/M, Thorlabs) via a magnet. The use of thin pellicle beam splitters eliminated the multiple reflections associated with plate beam splitters. The tooth pairs were adjustable in the occlusal, buccal and lingual views using translation and rotation tables. The NIR light reaching the sample transilluminated sound enamel but was scattered and reflected at caries lesions and dentin. The reflected NIR light was returned through the previously mentioned beam splitter to pass another linear polarizer (LPNIRE100-B, linear polarizer with N-BK7, 600–1100 nm, Thorlabs) and a longpass filter (FGL715M, 715 nm longpass filter, Thorlabs). The second polarizer, in combination with the first polarizer, reduced reflections from the glossy enamel surface in the image, whereas the longpass filter was used to remove undesired wavelengths below 715 nm caused by ambient light on the specimen. Images were obtained with an NIR camera (UI-124LE-NIR-DL, resolution 1280×1024, Imaging Development Systems GmbH, Obersulm, Germany) using a 50 mm lens (M118M50, Tamron, Saitama, Japan). The exposure times were 35–45 ms. One occlusal, one lingual and one buccal image were acquired per sample. All samples were photographed in a darkened room, and the setup was housed in a black box to reduce scattered light from the environment.

Digital BWR

The BWRs were obtained using a specially designed phantom that allowed X-ray of the samples with or without proximal contact points and the presence of antagonistic teeth to minimize the black background and ensure a clinically relevant grey value distribution.[3] All radiographs were taken using a Heliodent DS Dental X-ray unit (Sirona, Bensheim, Germany, 60 kV, 7 mA, 200 mm FHA cone, 0.08 s) and a digital charge-coupled device (CCD) sensor (Intra Oral II CCD sensor, Sirona, Bensheim, Germany, sensor dimensions 30.93 × 40.96 × 7.0 mm).

Micro-computed tomography

The samples were scanned using a fully shielded cone-beam desktop µCT scanner (µCT 40, Scanco Medical, Bassersdorf, Switzerland) operating at 70 kV and 114 µA with a 16.5 mm field of view. The scanning resolution was 512 × 512 points with a side length of the voxels of 32 µm for all axes. The plugin "KHKs_Scanco_ISQ_FileReader" was used to import the µCT data into Fiji for image processing.[25,26]

Calibration and training

Calibration, training and evaluation were conducted by an experienced trainer (K.H.K.) with 35 years of clinical and diagnostic research experience at various University Hospitals in Germany and by two dentist (K.H. and F.L.) with 14 and 9 years, respectively, of clinical diagnostic research experience at the University Hospital of Munich that included training of dental students in practical courses during this time. Instruction, evaluation and reliability assessment were conducted for each diagnostic method using images that were completely independent of the target pool of sample images that was analysed in this study. After theoretical instruction in the principles of all three diagnostic methods, exemplary images were explained and discussed in a training phase. Later, the examiners evaluated new sets of images in the presence of the trainer, and conflicting findings were discussed and agreed upon. The reliability assessment of the final evaluation phase resulted in agreement of greater than 90%.

Evaluation of findings

Evaluation of all findings was independently performed by the examiners in a darkened room (blinds were 2/3 closed, windows faced in a northern direction) on a calibrated monitor using the test pattern for the daily constancy test according to DIN 6868–157 with a seating distance of 60 cm (arm length) after at least 5 min of adaptation of the eyes to the room environment.[27] All assessments were performed in two evaluation cycles in randomized order with a minimum interval of two weeks and resulted in the achievement of a consensus for different ratings.

The 780 nm NIRR ($NIRR_{780nm}$) images from the occlusal, buccal and lingual views were evaluated as sound (0) or carious (1). A surface was considered diseased if a lighter area was detected in the proximal area within the sample. For evaluation from different directions, the proximal surface was classified as carious if the view from one direction achieved a score of 1; if all surfaces were scored 0, the whole sample was classified as healthy. The detectability of the enamel-dentin junction (EDJ) was evaluated from an occlusal perspective [no (0), yes (1)].

All 250 radiographs were scored according to the semiquantitative classification of Marthaler: absence of radiolucency (0), radiolucency in the outer or inner half of the enamel (1, 2) and radiolucency in the outer or inner half of the dentin (3, 4).[28] The µCT data were evaluated accordingly: absence of radiolucency (0), radiolucency in the outer half (1) or the inner half of the enamel (2) and radiolucency in the outer half (3) or the inner half of the dentin (4). As in our previously published work, we improved the evaluation by segmentation and centreline determination of the dentin and enamel in the 3D image.[3]

Table 1 Scoring of the test methods (NIRR and BWR) and the reference method (µCT) according to the criteria of sound or diseased surfaces

	Sound surface (0)	*Carious surface (1)*
NIRR occlusal	0	1
NIRR trilateral	0	1
BWR	0	1–4
µCT	0	1–4

Statistics

SAS/STAT software (SAS/STAT, v.15.1, Cary, NC, USA) using the Proc Power procedure was used for sample size calculation. Statistical analysis was conducted using the statistical software SPSS (IBM SPSS Statistics for Windows, v.25.0, Armonk, NY, USA) and comprised the calculation of sensitivity, specificity and area under the curves (AUCs). Overall accuracy was calculated as the number of correctly classified sites divided by the total number of reference sites and expressed as a percentage. Likewise, overestimation was calculated as the number of false-positive (FP) values divided by the number of reference sites, and underestimation was calculated as the number of false-negative (FN) values divided by the number of reference sites. A cross-table was used to compare NIRR and BWR ratings with those obtained using µCT. Table 1 shows the scorings of the test and reference methods according to the criteria for sound and diseased classifications. Multiple comparisons of AUCs within the thresholds were performed using easyROC and the Bonferroni method.[29] Interpretation of the AUC values was 0.5 = no discrimination; 0.5–0.7 = poor to fair discrimination; 0.7–0.8 = acceptable discrimination; 0.8–0.9 = excellent discrimination and AUC ≥0.9 = outstanding discrimination.[30] Reliability assessments for $NIRR_{780nm}$ and BWRs were calculated using linearly weighted Cohen's κ (wκ), where a 1-category difference was considered less severe than a 2-category difference.[31] The two-sided significance level was set at $\alpha = 0.05$ for all tests.

Results

Nearly perfect agreement between the examiners was achieved for determination of the reference standard using µCT imaging (wκ 0.99, confidence interval (CI): 0.97–1.00). The scores obtained in the occlusal and trilateral $NIRR_{780nm}$ assessments as well as the BWR

Table 2 Cross-table of ratings for NIRR from occlusal or trilateral views and for digital BWR with corresponding ratings based on µCT. Images that were not assessable are marked "na" (not applicable)

		NIRR occlusal		*NIRR trilateral*		*BWR*						
		0	*1*	*0*	*1*	*0*	*1*	*2*	*3*	*4*	*na*	*Total*
µCT	0	133	25	110	48	154	0	0	0	0	4	158
	1	14	5	8	11	19	0	0	0	0	0	19
	2	21	8	11	18	23	2	2	1	0	1	29
	3	28	14	14	28	24	4	7	6	0	1	42
	4	2	0	1	1	0	0	1	0	1	0	2
	Total	198	52	144	106	220	6	10	7	1	6	250

assessment compared with µCT as a reference test are shown in Table 2. The inter-rater reliability assessment (wκ) showed almost perfect agreement for $NIRR_{780nm}$, trilateral $NIRR_{780nm}$ and BWR (wκ 0.85–0.95), and the values for intra-rater reliability showed almost perfect agreement for BWR (wκ 0.90–0.91) and substantial agreement for $NIRR_{780nm}$ and trilateral $NIRR_{780nm}$ (wκ 0.74–0.78).[32] An overall accuracy of 63.1 %, an underestimation of 32.8% and an overestimation of 0.4% were found for BWR. Occlusal $NIRR_{780nm}$ images achieved an overall accuracy of 64.0%, an underestimation of 26.0% and an overestimation of 10.0%. The merged results of the trilateral $NIRR_{780nm}$ assessment exhibited an overall accuracy of 67.2 %, an underestimation of 13.6% and an overestimation of 19.2%. Detection of the EDJ using $NIRR_{780nm}$ was possible in 55 (22.2 %) samples, 49.1% of premolars and 14.0% of molars (χ^2 $p < 0.001$). High specificity values were found for $NIRR_{780nm}$ and BWR, with slightly poorer results for $NIRR_{780nm}$. When premolars and molars were analysed separately, values for specificity remained consistently high. The sensitivity values for $NIRR_{780nm}$ and BWR were similarly low. Only for $NIRR_{780nm}$ including the findings for all surfaces were the sensitivity values in the same range as the specificity values (Table 3). The AUC values for all test methods are shown in Table 3 and Figure 2. Multiple comparisons of AUCs showed no significant difference between $NIRR_{780nm}$ and BWR, and there was also no statistically significant difference between the methods within tooth type groups ($p < 0.05$).

Discussion

This study investigated the potential of NIRR below 800 nm when operated under ideal laboratory conditions to detect early proximal caries lesions in permanent molars and premolars with comparable diagnostic accuracy to BWR, as BWR is the method most commonly used as an adjunct to visual-tactile examination in caries detection. For the analysis, an *in vitro* model that made trilateral $NIRR_{780nm}$ assessment from the occlusal, buccal and lingual sides of the teeth possible was developed, and µCT was used as a reference standard. As the main result of this study, it can be stated that NIRR and BWR showed comparable results in diagnostic

Table 3 Sensitivity, specificity, false-positive (FP) value, false-negative (FN) value and area under the curve (AUC) for NIRR from the occlusal and trilateral views as well as for digital BWR with µCT as the reference test (lower and upper 0.95 CI in parentheses) for caries lesions

		Sensitivity	*Specificity*	*FP*	*FN*	*AUC*
NIRR occlusal	All teeth	0.29 (0.20–0.39)	0.84 (0.78–0.90)	0.16 (0.10–0.22)	0.71 (0.61–0.77)	0.57 (0.49–0.64)
	Premolar	0.39 (0.24–0.55)	0.84 (0.68–1.01)	0.16 (-0.01–0.32)	0.61 (0.45–0.76)	0.62 (0.47–0.77)
	Molar	0.22 (0.11–0.33)	0.84 (0.78–0.90)	0.16 (0.10–0.22)	0.78 (0.67–0.84)	0.53 (0.44–0.62)
NIRR trilateral	All teeth	0.63 (0.53–0.73)	0.70 (0.62–0.77)	0.30 (0.23–0.38)	0.37 (0.27–0.45)	0.66 (0.59–0.73)
	Premolar	0.66 (0.51–0.81)	0.53 (0.30–0.75)	0.47 (0.25–0.70)	0.34 (0.19–0.54)	0.59 (0.43–0.75)
	Molar	0.61 (0.48–0.74)	0.72 (0.64–0.79)	0.28 (0.21–0.36)	0.39 (0.26–0.48)	0.67 (0.58–0.75)
BWR	All teeth	0.27 (0.17–0.36)	1.00 (1.00–1.00)	0.00 (0.00–0.00)	0.73 (0.64–0.80)	0.63 (0.55–0.70)
	Premolar	0.33 (0.18–0.49)	1.00 (1.00–1.00)	0.00 (0.00–0.00)	0.67 (0.51–0.81)	0.65 (0.50–0.80)
	Molar	0.22 (0.11–0.33)	1.00 (1.00-.100)	0.00 (0.00–0.00)	0.78 (0.67–0.84)	0.60 (0.50–0.69)

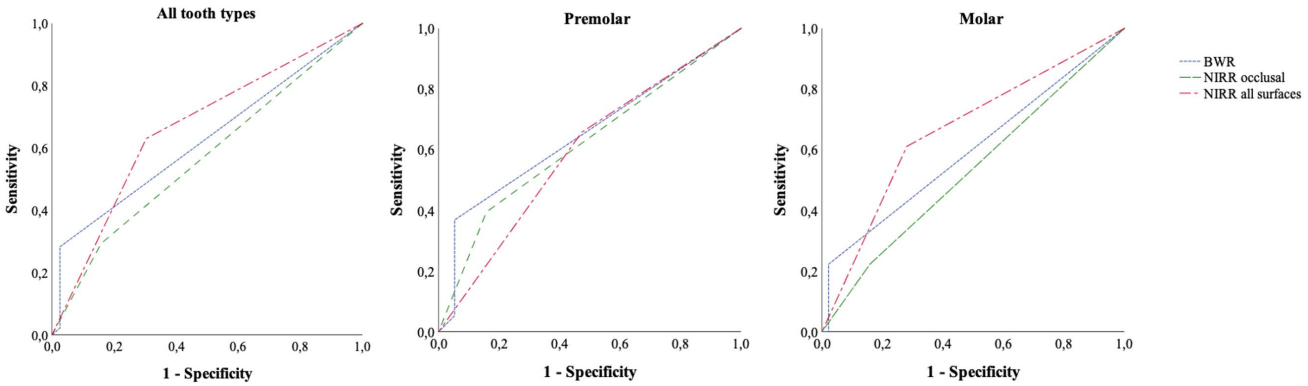

Figure 2 Receiver operating characteristic curves for caries lesions for all tooth types and for teeth separated into premolar and molar groups. Equal areas under the curve were observed for BWR, NIRR from the occlusal view and NIRR combined with all views ($p > 0.05$).

performance, with a generally deficient potential for detecting enamel caries lesions and low sensitivity and high specificity for the detection of proximal caries in general.

NIRR should not be confounded with near-infrared transillumination (NIRT), as they are quite different methods. Although both methods use NIR light to visualize caries lesions, they differ in the optical principles on which they are based. In both methods, NIR light is scattered by carious enamel; in the case of NIRR, this results in a stronger reflection back to the sensor. As a result, the local light intensity at a carious lesion is increased compared to that at the adjacent healthy enamel, causing caries to appear brighter than the healthy surrounding enamel in the NIRR image. In contrast, caries lesions appear dark with NIRT because less light reaches the detector due to light scattering in the decayed area.

In NIRT, the scattering of light within the dentin makes the dentin core appear as a homogeneous light source that uniformly illuminates the entire tooth surface from the inside. Thus, caries lesions that are located between the dentin core and the tooth surface can be efficiently detected.[10] In comparison, NIRR does not reflect light uniformly at the dentin core; the amount of reflected light depends on the angle between the incident light and the dentin surface. When NIR light is perpendicularly incident to the surface, the amount of reflected light reaches a maximum. When the light hits the dentin surface at small angles, for example, at the proximal surface of the tooth, only a small amount of light is reflected. The amount of reflected light is proportional to the cosine of the angle between the incident light and the dentin surface. Thus, the different results of previous studies can also be explained, as NIRT achieves satisfactory results in proximal caries detection, while NIRR achieves poorer results and low sensitivity.[10–12,15]

Although NIR light of wavelength 1300 nm passes through healthy enamel with marginal scattering, 1300 nm is the optimal imaging wavelength for achieving a balance between the attenuation of enamel and that of water. However, commercially available devices for transillumination operate at a wavelength of 780 nm, while those using reflection operate at 850 nm.[10,15,18] The most likely reasons for this are, first, that there are patents for transillumination devices that operate in the wavelength range of 795 to 1600 nm, although they do not cover NIRR.[33] Second, the use of wavelengths above 850 nm requires a camera with an indium-gallium-arsenide sensor. These sensors are still rather expensive and, therefore, are probably not currently being considered by manufacturers for inclusion in commercial devices.[34] Hence, few studies are available on the diagnostic performance of NIRR above 1000 nm.[35] Due to the limitations described, only the low NIR range around 780 nm has currently been applied in optical diagnostic methods for caries detection in routine clinical work.

The μCT, the reference standard used in this analysis, has been proven to be a valid method for determining the actual extent of caries within a sample tooth without destroying it.[36–38] Based on the three-dimensional information provided by μCT, the proportional distance between the EDJ and the contours of the pulp chamber can be determined, and the extent of a carious lesion can be precisely located. Studies involving a comparatively large number of samples in which the diagnosis was confirmed by histology or μCT are rare. This is one advantage of the present study, as μCT is a cost-intensive procedure, and, to our knowledge, there are currently no other studies based on a comparably large sample pool validated by μCT.

The use of μCT and NIRR as well as BWR had no adverse effects on the samples. The low levels of ionizing radiation used in μCT and BWR have no impact on the tooth structure. Care was also taken to ensure that the stored samples were covered with sufficient solution, and the period of time during which they were removed from the solution for examination was kept short enough to prevent the samples from drying out. In this way, cracks and discolouration due to incorrect storage were avoided.

Special care was taken to select samples suitable for this study and to use a statistically sufficient sample

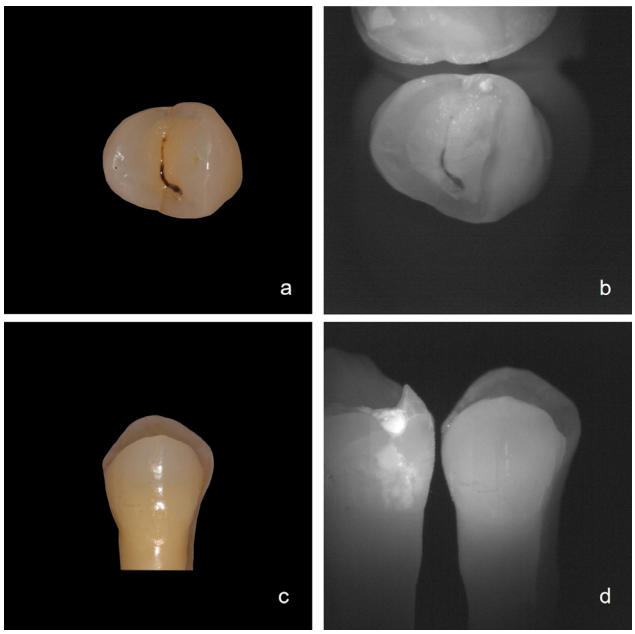

Figure 3 A premolar with a proximal non-cavitated caries lesion. (a) In the clinical occlusal view, no caries lesion was detectable. (b) In the occlusal view with NIRR, a white spot was visible in the area of the marginal ridge. A white rim could be observed around the tooth in the marginal ridge region. (c) No signs of demineralization or caries were visible in the clinical view from the lingual side. (d) In the lingual view using NIRR, no signs of caries or demineralization were visible, although demineralization was observed as white specks on the adjacent molar.

size. Caries prevalence was not estimated according to a purely epidemiological background as in surveys such as "The Fifth German Oral Health Study (DMS V)".[39]

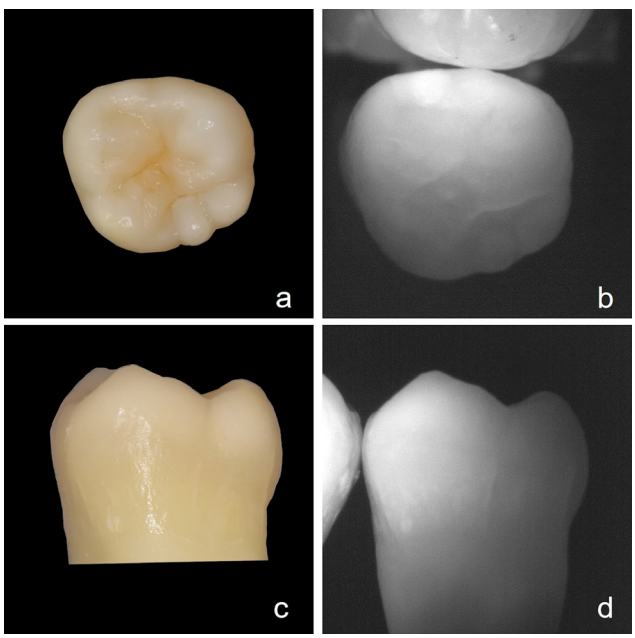

Figure 4 Caries detection with NIRR was impossible in a molar with opaque enamel.

In such epidemiological surveys, the general prevalence of non-cavitated caries lesions probably remains underestimated. Since this study focused on detecting even non-cavitated early proximal enamel and dentin lesions, the number of advanced dentin lesions was underrepresented within the test sample. A caries prevalence of 50% was a realistic and appropriate composition for obtaining statistically significant data, and this has been confirmed in the literature.[40] The calculated sample size of 250 yields representative results; however, the results of this analysis should be interpreted in the context of the composition of our sample and its size. Because the focus of this study was detection of early caries, the selection of teeth with caries lesions focused on non-cavitated enamel and dentin lesions. It is not clear whether the presence of a higher proportion of advanced lesions within our sample would have improved or worsened diagnostic accuracy. Due to its physical properties and depth of penetration, NIRR cannot detect dentin caries. Similarly, cavitations can negatively affect diagnostic performance, and this could lead to a bias in our results. Consequently, the results of this diagnostic study using $NIRR_{780nm}$ can be applied only to the detection of early proximal caries.

For comparison with the $NIRR_{780nm}$ images, BWRs were taken in a phantom that can be used to mimic the setting in which standard BWRs are obtained. In our previous studies, we showed that approximately only 20% of all clinical BWRs with proximal contact are free of superimpositions. To avoid compromising the diagnostic potential of BWR by superposition artefacts, we performed BWR using a phantom without proximal contact. In this way, lesions that can be radiographically imaged can be assessed as accurately as is technically possible.[3] The sensitivity value of 27% for caries detection using BWRs in this analysis was low; low sensitivity of BWR is not unexpected and has been frequently described in the literature, as the mineral loss at enamel lesions is often too low to be visualized in BWRs. In general, large enamel defects or dentin caries can be detected by BWR with high sensitivity.[8,23] However, many studies have shown that BWRs have a specificity greater than 90%, making them a suitable standard for comparison with results of $NIRR_{780nm}$.[23]

In contrast, for the NIRR images, it is imperative to simulate adjacent tooth contact to create clinically relevant conditions for diagnosis; this could be sufficiently achieved in our experimental setup.

Using our laboratory setup, which included the use of coaxial illumination, polarization filters and calibrated diagnostic monitors, we were able to create optimal conditions for NIRR analysis. Polarizing filters were used to reduce reflection artefacts due to the specular tooth surface.[41,42] Light reflections can be responsible for poor diagnostic discrimination because they limit the greyscale range for caries detection due to the automatic exposure correction of most camera systems.[15] Automatic exposure algorithms are usually

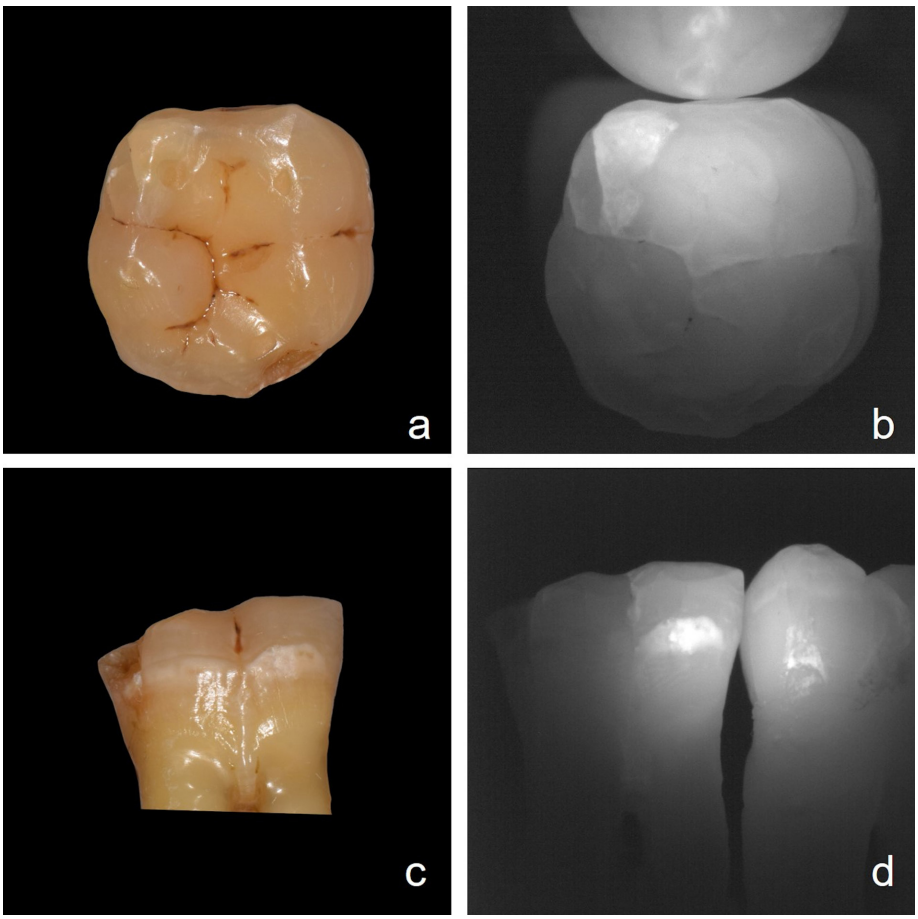

Figure 5 A molar with circumferential demineralization (c and d). The crack in the mesio-lingual cusp became visible using NIRR (a and b).

based on the brightest and darkest pixels and divide this measurement range into 256 grey levels, as in the case of 8-bit greyscale images. When a large brightness range is covered, small differences fall into a few pixel bins. In addition, since the eye can distinguish approximately only 60 shades of grey, it is possible that the grey level differences relevant to caries detection are too small to be perceived clinically. A remedy for this would be the use of high dynamic range (HDR) images. However, these require approximately 40 ms of time per image. If several images must be captured for an HDR recording, the recording time increases, and this can result in motion blur due to camera shake in freehand recordings. Blurring reduces the spatial resolution in a way analogous to a blur filter and has a negative influence on the detection of small structures, for example, initial defects. The problems described here using 8-bit images as an example also apply to a large extent to images obtained using 12- and 16-bit sensors.[43] A substantial reduction in these reflection artefacts was successfully realized by our experimental setup, but the diagnostic performance of NIRR in the wavelength range of approximately 780 nm was not improved.

Another advantage of our experimental setup is the use of coaxial illumination, which was achieved through the use of a beam splitter. In contrast, optical diagnostic systems currently on the market position the illumination elements next to the camera for reasons related to space and cost and do not use a beam splitter. The lateral arrangement of the light source results in unilateral shadowing due to the triangulation angle of the light source-tooth surface-camera. As a result, because the reflection depends on the angle of incidence, the incident NIR light is not reflected uniformly by the dentin core. In addition, the neighbouring tooth blocks some of the NIR light if the light source is mounted next to the sensor. Coaxial illumination avoids these problems. Despite the optimal conditions, $NIRR_{780nm}$ only sufficiently distinguished between enamel and dentin tissue or depicted the EDJ, especially in the proximal region, in 55 of 250 samples. Our data were confirmed in 2017 by Jablonski-Momeni et al., who also observed poor potential of NIRR to discriminate the enamel at 850 nm.[12] Furthermore, we observed that differentiation of the EDJ was significantly better in premolars than in molars, likely due to the presence of a thinner enamel layer in premolars or to the size or radius of the proximal contact surface. Contrast decreases significantly with increasing enamel thickness.[18] We did not classify caries as a function of the distance between the pulp

and the enamel and dentin because it was simply not possible to reliably discriminate between enamel and dentin. Consequently, the $NIRR_{780nm}$ findings were only dichotomously differentiated into healthy or diseased. A more detailed classification of lesion severity would probably be possible in higher NIR ranges of approximately 1300 nm, as the attenuation coefficient of enamel decreases with increasing wavelength, and at higher wavelengths enamel visually appears more translucent. The evaluation of dichotomous $NIRR_{780nm}$ findings, in addition to the use of a comprehensive training and calibration process, may also explain the high reliability assessment scores we observed for $NIRR_{780nm}$.

The detection of early proximal caries with $NIRR_{780nm}$ and BWR showed comparable outcomes. However, BWR evaluation resulted in a more pronounced underestimation of caries (32.8 %) and a comparatively low overestimation (0.4 %), while $NIRR_{780nm}$ showed high underestimation (26.0 %) as well as relatively high overestimation of 15.8% in the occlusal view. In the trilateral view with $NIRR_{780nm}$, underestimation decreased slightly (13.6 %), but overestimation increased to 19.2%. The high FP rate obtained with $NIRR_{780nm}$ is the major obstacle to its possible transfer to clinical practice. The overestimation rate obtained using $NIRR_{780nm}$ is inconsistent with the goal of preventive and non-invasive dentistry and might lead to invasive overtreatment.

The FP diagnostic decisions were probably caused by artefacts present in numerous $NIRR_{780nm}$ images, as a white rim could be observed in some $NIRR_{780nm}$ images around the tooth in the marginal ridge region (Figure 3). This phenomenon is suspected to be due to the surface curvature of the marginal ridge. The slope of the enamel surface influences the direction in which the light reflected from the dentin core is diffracted.[15] The presence of this white rim made it difficult to detect caries in the outer part of the enamel, since the two areas overlapped in the projection onto the camera. It is therefore easier to fail to identify caries when evaluating images of this area. Another possible reason for the high FP rate of the trilateral $NIRR_{780nm}$ assessment, in particular, is staining. It has been reported that light below 1100 nm, especially light at 780 nm, is absorbed by coloured pigments.[44] This absorption contributes more to lesion contrast than does the increased scattering due to demineralization.[19] Although these artefacts are a potential source of error, they are not responsible for the poor diagnostic performance of $NIRR_{780nm}$ in this study, as our samples showed little discolouration.

The opacity of the enamel tissue also influences the detection of caries. For example, highly opaque enamel renders the detection of caries more difficult or even impossible (Figure 4). The descriptive term "opaque" corresponds physically to greater light scattering. If the entire enamel scatters light more, it is difficult to distinguish the brightness caused by initial caries from the inherent brightness of the normal enamel. Studies using NIRT have already described this phenomenon.[13,45]

Clinically, it is possible to inspect the tooth not only from the occlusal side-but also from the buccal and lingual sides. Combining the buccal and lingual views under $NIRR_{780nm}$ conditions did not improve the accuracy of caries detection in the proximal region compared to evaluation based on the occlusal view alone, but it did increase the overestimation of caries, likely due to the presence of superficial decalcifications in the buccal and lingual areas, which are projected into the proximal caries area in the image and are also very bright under $NIRR_{780nm}$ illumination. This prevents detection of the extent of an underlying lesion.

NIR light at 1300 nm can be used to visualize early demineralization by reflection since the contrast between healthy and demineralized enamel is greatest due to the minimal scattering of sound enamel.[46] Even at 780 nm, it is possible to detect early demineralization on the buccal or lingual and occlusal surfaces, while this is more difficult proximally due to the above-mentioned artefacts (Figure 5).

In this analysis, we made observations that suggest further interesting uses of NIRR. Cracks, the extent of which is difficult to estimate by visual examination, were visualized by our *in vitro* model (Figure 5). The validity of this capability can be the focus of future research.

The hypothesis that short-wavelength NIRR (<800 nm) cannot detect early proximal caries lesions with high sensitivity and specificity (>70 %) was confirmed. The second hypothesis was rejected because $NIRR_{780nm}$ yielded diagnostic results comparable in sensitivity and specificity to those obtained using BWR. However, when interpreting these results, it is important to note that the proportion of false positives was significantly higher with $NIRR_{780nm}$ than with BWR. Additionally, trilateral $NIRR_{780nm}$ assessment did not provide any further advantages for diagnostic performance compared to assessment from the occlusal view alone. Furthermore, overestimation of the presence of caries lesions represents a severe disadvantage of $NIRR_{780nm}$ and limits its applicability in clinical practice.

Although short-wavelength $NIRR_{780nm}$ is not suitable for the reliable detection of noncavitated proximal caries, its potential for use in identifying healthy proximal surfaces with high specificity is apparent. An advantage of NIRR over BWR is that no ionizing radiation is used, allowing monitoring of lesions without harming tissues. The results of this study demonstrate that NIRR, even NIRR using wavelengths below 800 nm, has the potential to reduce patients' exposure to ionizing radiation in routine clinical practice.

Conclusion

Despite the use of an ideal optical setup and optimized conditions, NIRR at lower wavelengths appears to be an unsatisfactory method for the detection of early proximal caries. Although its diagnostic performance was comparable to that of BWR, $NIRR_{780nm}$ did not have

the potential to discriminate between enamel and dentin tissues and exhibited a high risk of overestimation of the presence of proximal caries lesions.

Funding

Open Access funding enabled and organized by ProjektDEAL.

REFERENCES

1. Schwendicke F, Splieth C, Breschi L, Banerjee A, Fontana M, Paris S, et al. When to intervene in the caries process? an expert Delphi consensus statement. *Clin Oral Investig* 2019; **23**: 3691–703. doi: https://doi.org/10.1007/s00784-019-03058-w
2. Young DA, Featherstone JDB. Caries management by risk assessment. *Community Dent Oral Epidemiol* 2013; **41**: e53–63. doi: https://doi.org/10.1111/cdoe.12031
3. Heck K, Litzenburger F, Ullmann V, Hoffmann L, Kunzelmann K-H. In vitro comparison of two types of digital X-ray sensors for proximal caries detection validated by micro-computed tomography. *Dentomaxillofac Radiol* 2020; **0**: 20200338. doi: https://doi.org/10.1259/dmfr.20200338
4. Künisch J, Schaefer G, Pitchika V, Garcia-Godoy F, Hickel R. Evaluation of detecting proximal caries in posterior teeth via visual inspection, digital bitewing radiography and near-infrared light transillumination. *Am J Dent* 2019; **32**: 74–80.
5. Kocak N, Cengiz-Yanardag E. Clinical performance of clinical-visual examination, digital bitewing radiography, laser fluorescence, and near-infrared light transillumination for detection of non-cavitated proximal enamel and dentin caries. *Lasers Med Sci* 2020; **35**: 1621–8. doi: https://doi.org/10.1007/s10103-020-03021-2
6. Poorterman JH, Aartman IH, Kalsbeek H. Underestimation of the prevalence of approximal caries and inadequate restorations in a clinical epidemiological study. *Community Dent Oral Epidemiol* 1999; **27**: 331–7. doi: https://doi.org/10.1111/j.1600-0528.1999.tb02029.x
7. Pitts NB, Rimmer PA. An in vivo comparison of radiographic and directly assessed clinical caries status of posterior approximal surfaces in primary and permanent teeth. *Caries Res* 1992; **26**: 146–52. doi: https://doi.org/10.1159/000261500
8. Espelid I, Tveit AB. Radiographic diagnosis of mineral loss in approximal enamel. *Caries Res* 1984; **18**: 141–8. doi: https://doi.org/10.1159/000260762
9. Hwang S-Y, Choi E-S, Kim Y-S, Gim B-E, Ha M, Kim H-Y. Health effects from exposure to dental diagnostic X-ray. *Environ Health Toxicol* 2018; **33**: e2018017. doi: https://doi.org/10.5620/eht.e2018017
10. Lederer A, Kunzelmann K-H, Heck K, Hickel R, Litzenburger F. In vitro validation of near-infrared transillumination at 780 nm for the detection of caries on proximal surfaces. *Clin Oral Investig* 2019; **23**: 3933–40. doi: https://doi.org/10.1007/s00784-019-02824-0
11. Lederer A, Kunzelmann KH, Hickel R, Litzenburger F. Transillumination and HDR imaging for proximal caries detection. *J Dent Res* 2018; **97**: 844–9. doi: https://doi.org/10.1177/0022034518759957
12. Jablonski-Momeni A, Jablonski B, Lippe N. Clinical performance of the near-infrared imaging system VistaCam iX Proxi for detection of approximal enamel lesions. *BDJ Open* 2017; **3**: 17012. doi: https://doi.org/10.1038/bdjopen.2017.12
13. Abdelaziz M, Krejci I. DIAGNOcam-a near infrared digital imaging transillumination (NIDIT) technology. *Int J Esthet Dent* 2015; **10**: 158–65.
14. Abdelaziz M, Krejci I, Perneger T, Feilzer A, Vazquez L. Near infrared transillumination compared with radiography to detect and monitor proximal caries: a clinical retrospective study. *J Dent* 2018; **70**: 40–5. doi: https://doi.org/10.1016/j.jdent.2017.12.008
15. Lederer A, Kunzelmann K-H, Heck K, Hickel R, Litzenburger F. In-Vitro validation of near-infrared reflection for proximal caries detection. *Eur J Oral Sci* 2019; **127**: 515–22. doi: https://doi.org/10.1111/eos.12663
16. Fried D, Glena RE, Featherstone JD, Seka W. Nature of light scattering in dental enamel and dentin at visible and near-infrared wavelengths. *Appl Opt* 1995; **34**: 1278–85. doi: https://doi.org/10.1364/AO.34.001278
17. Fried D, Featherstone JDB, Darling CL, Jones RS, Ngaotheppitak P, Bühler CM. Early caries imaging and monitoring with near-infrared light. *Dent Clin North Am* 2005; **49**: 771–93. doi: https://doi.org/10.1016/j.cden.2005.05.008
18. Jones R, Huynh G, Jones G, Fried D. Near-Infrared transillumination at 1310-nm for the imaging of early dental decay. *Opt Express* 2003; **11**: 2259–65. doi: https://doi.org/10.1364/OE.11.002259
19. Ng C, Almaz E, Simon J, Fried D, Darling C. Near-Infrared imaging of demineralization on the occlusal surfaces of teeth without the interference of stains. *J Biomed Opt* 2019; **24**: 036002. doi: https://doi.org/10.1117/1.JBO.24.3.036002
20. Litzenburger F, Lederer A, Kollmuß M, Hickel R, Kunzelmann K-H, Heck K. Near-Infrared transillumination with high dynamic range imaging for occlusal caries detection in vitro. *Lasers Med Sci* 2020; **35**: 2049–58. doi: https://doi.org/10.1007/s10103-020-03078-z
21. Lee C, Lee D, Darling CL, Fried D. Nondestructive assessment of the severity of occlusal caries lesions with near-infrared imaging at 1310 nm. *J Biomed Opt* 2010; **15**: 047011. doi: https://doi.org/10.1117/1.3475959
22. Hirasuna K, Fried D, Darling CL. Near-Infrared imaging of developmental defects in dental enamel. *J Biomed Opt* 2008; **13**: 044011. doi: https://doi.org/10.1117/1.2956374
23. Schwendicke F, Tzschoppe M, Paris S. Radiographic caries detection: a systematic review and meta-analysis. *J Dent* 2015; **43**: 924–33. doi: https://doi.org/10.1016/j.jdent.2015.02.009
24. Banting D, Eggertsson H, Ekstrand K, Ferreira-Zandoná A, Ismail A, Longbottom C. Rationale and evidence for the International caries detection and assessment system (ICDAS II). *Ann Arbor* 2005; **1001**: 48109–41078.
25. Schindelin J, Arganda-Carreras I, Frise E, Kaynig V, Longair M, Pietzsch T, et al. Fiji: an open-source platform for biological-image analysis. *Nat Methods* 2012; **9**: 676–82. doi: https://doi.org/10.1038/nmeth.2019
26. Kunzelmann KH. ImageJ I/O utilities. 2012. Available from: http://www.kunzelmann.de/6_software-imagej-import-export-utilities.html.
27. DIN Deutsches Institut für Normung e.V. Normenausschuss Radiologie (NAR).2014.Sicherung der Bildqualität in röntgendiagnostischen Betrieben - Teil 157: Abnahme- und Konstanzprüfung nach RöV an Bildwiedergabesystemen in ihrer Umgebung
28. Marthaler TM. A standardized system of recording dental conditions. *Helv Odontol Acta* 1966; **10**: 1–18.
29. Goksuluk D, Korkmaz S, Zararsiz G, Karaagaoglu A.,Ergun. easyROC: an interactive web-tool for ROC curve analysis using R language environment. *R J* 2016; **8**: 213–20. doi: https://doi.org/10.32614/RJ-2016-042
30. Hosmer DW, Lemeshow S. *Applied logistic regression. 2nd ed.* New York: Wiley; 2000. pp. 156–64.
31. Cohen J. Weighted kappa: nominal scale agreement with provision for scaled disagreement or partial credit. *Psychol Bull* 1968; **70**: 213–20. doi: https://doi.org/10.1037/h0026256
32. Landis JR, Koch GG. The measurement of observer agreement for categorical data. *Biometrics* 1977; **33**: 159–74. doi: https://doi.org/10.2307/2529310

33. Fried D, Jones R. *InventorsNear-infrared transillumination for the imaging of early dental decay. United States patent. 20060223032*; 2006.
34. Jones GC, Jones RS, Fried D. Transillumination of interproximal caries lesions with 830-nm light.. In: Rechmann P, Fried D, Hennig T, eds.*Lasers in Dentistry X*: SPIE; 2004. https://doi.org/10.1117/12.539289. doi: https://doi.org/10.1117/12.539289
35. Simon JC, Lucas SA, Staninec M, Tom H, Chan KH, Darling CL, et al. Near-IR transillumination and reflectance imaging at 1,300 nm and 1,500-1,700 nm for in vivo caries detection. *Lasers Surg Med* 2016; **48**: 828–36. doi: https://doi.org/10.1002/lsm.22549
36. Boca C, Truyen B, Henin L, Schulte AG, Stachniss V, De Clerck N, et al. Comparison of micro-CT imaging and histology for approximal caries detection. *Sci Rep* 2017; **7**: 6680. doi: https://doi.org/10.1038/s41598-017-06735-6
37. Özkan G, Kanli A, Başeren NM, Arslan U, Tatar İlkan, Tatar I. Validation of micro-computed tomography for occlusal caries detection: an in vitro study. *Braz Oral Res* 2015; **29**: S1806–83242015000100309. doi: https://doi.org/10.1590/1807-3107BOR-2015.vol29.0132
38. Soviero VM, Leal SC, Silva RC, Azevedo RB. Validity of MicroCT for in vitro detection of proximal carious lesions in primary molars. *J Dent* 2012; **40**: 35–40. doi: https://doi.org/10.1016/j.jdent.2011.09.002
39. Jordan RA, Bodechtel C, Hertrampf K, Hoffmann T, Kocher T, Nitschke I, et al. The fifth German oral health study (Fünfte Deutsche Mundgesundheitsstudie, DMS V) - rationale, design, and methods. *BMC Oral Health* 2014; **14**: 161. doi: https://doi.org/10.1186/1472-6831-14-161
40. Jacobsen ID, Crossner C-G, Eriksen HM, Espelid I, Ullbro C. Need of non-operative caries treatment in 16-year-olds from Northern Norway. *Eur Arch Paediatr Dent* 2019; **20**: 73–8. doi: https://doi.org/10.1007/s40368-018-0387-z
41. Benson PE, Ali Shah A, Robert Willmot D. Polarized versus nonpolarized digital images for the measurement of demineralization surrounding orthodontic brackets. *Angle Orthod* 2008; **78**: 288–93. doi: https://doi.org/10.2319/121306-511.1
42. Everett MJ, Colston Jr BW, Sathyam US, Da Silva LB, Fried D, Featherstone JD. Noninvasive diagnosis of early caries with polarization-sensitive optical coherence tomography (PS-OCT. *International Society for Optics and Photonics* 1999; **3593**: 177–82.
43. Reinhard E, Heidrich W, Debevec P, Pattanaik S, Ward G, Myszkowski K. High dynamic range imaging: acquisition, display, and image-based lighting: Morgan Kaufmann. 2010;.
44. Almaz EC, Simon JC, Fried D, Darling CL. Influence of stains on lesion contrast in the pits and fissures of tooth occlusal surfaces from 800-1600-nm. *Proc SPIE Int Soc Opt Eng* 2016; **9692**: 96920X. doi: https://doi.org/10.1117/12.2218663
45. Söchtig F, Hickel R, Kühnisch J. Caries detection and diagnostics with near-infrared light transillumination: clinical experiences. *Quintessence Int* 2014; **45**: 531–8. doi: https://doi.org/10.3290/j.qi.a31533
46. Darling CL, Huynh GD, Fried D. Light scattering properties of natural and artificially demineralized dental enamel at 1310 nm. *J Biomed Opt* 2006; **11**: 034023. doi: https://doi.org/10.1117/1.2204603